Atmos. Meas. Tech. Discuss., 8, 8903–8923, 2015
www.atmos-meas-tech-discuss.net/8/8903/2015/
doi:10.5194/amtd-8-8903-2015

Atmospheric Measurement Techniques Discussions
Open Access

Estimating of total atmospheric water vapor content from MSG1-SEVIRI observations

A. Labbi and A. Mokhnache

Department of physics, Faculty of Exact Sciences, University of Constantine 1, Constantine 25017, Algeria

Received: 3 August 2015 – Accepted: 19 August 2015 – Published: 28 August 2015

Correspondence to: A. Labbi (labbiabdelkader@yahoo.fr)

Published by Copernicus Publications on behalf of the European Geosciences Union.

Abstract

In this work, we proposed a methodology to estimate total atmospheric water vapor content (TAWV) from observations of the Spinning Enhanced Visible and Infrared Imager (SEVIRI) on board the first Meteosat Second Generation satellite (MSG1). The method used is called the split-window technique which requires only the data from the channels IR10.8 and IR12, therefore this method not requires any ancillary data. This method is based on the MSG1 observations of the same geographic location over land at two slightly different times during a period when the ground temperature is changing rapidly. The main contribution of the present work is to consider that the relationship between TAWV and the ratio of the two split-window channel transmittances ($\tau_{12}/\tau_{10.8}$) is a quadratic formula, this assumption is based on the "Roberts" approach simulations using MSG1-SEVIRI filter response functions for a 2311 atmospheric situations from the TIGR dataset. For validation, we have examined the accuracy of the TAWV estimated in this work by comparison with the data obtained from radiosonde and from aerosol robotic network (AERONET). On the one hand, the comparison with the radiosonde data show that the root mean square error (RMSE) equals $0.66\,\mathrm{g\,cm^{-2}}$, the standard deviation (SD) equals $0.59\,\mathrm{g\,cm^{-2}}$ and the correlation coefficient (R) equals 0.79. On the other hand, the comparison with the AERONET data show that the RMSE equals $0.42\,\mathrm{g\,cm^{-2}}$, the SD equals $0.29\,\mathrm{g\,cm^{-2}}$ and the R equals 0.82. Also, the comparison with another method demonstrates that the spatial variation of TAWV here is reasonable. We have concluded in this study that the TAWV can be determined from the MSG1-SEVIRI observations with accuracy acceptable which can be used for climate change research.

1 Introduction

Total atmospheric water vapor content (TAWV) is an important factor in atmospheric correction of high spatial resolution satellite data and it also strongly required for the improvement of the precision of land surface temperature estimates obtained from satellite thermal infrared data (Zhang et al., 2008; Price, 1983). Therefore, it is required for a wide variety of climatic, hydrological, ecological, and biogeochemical studies. TAWV can be defined as the amount of vertically integrated water vapor and can be expressed in cm or in $\mathrm{g\,cm^{-2}}$ (Morales-Salinas et al., 2012).

Spatial variations of TAWV can be measured and mapped using the observations of the Spinning Enhanced Visible and Infrared Imager (SEVIRI) on board the first Meteosat Second Generation satellite (MSG1) (Schroedter-Homscheidt et al., 2008). A number of algorithms have been proposed to derive TAWV from satellite observations in thermal infrared and can be classified as following: simple split-window of thermal channels (Dalu, 1986), variance ratio (Jedlovec, 1990), regression slope (Goward et al., 1994), covariance–variance method and look-up table approach (Czaglowski et al., 2002), linear atmosphere–surface temperature relationship (Sobrino et al., 2002).

In this paper, the technique called split-window has been used. This technique was originally derived for the estimation of sea surface temperature from satellite (Anding and Kauth, 1970), which makes use of two differentially absorbing channels in the thermal infrared spectral region (10.5–12.5 µm) to remove the contaminating effect of water vapor and thus arrives at an improved estimate of the sea or land surface temperature. In this technique, for estimating the TAWV from MSG1-SEVIRI, we can use the MSG1 observations of the same geographic location over land at two slightly different times during a period when the ground temperature is changing rapidly (Schroedter-Homscheidt et al., 2008). For more detailed and discussion of the split-window technique see the reference (Kleespies and McMillin, 1990).

The main purpose of the present study is to consider that the relation between TAWV and the ratio of the two split-window channel transmittances ($\tau_{12}/\tau_{10.8}$) is a quadratic

AMTD
8, 8903–8923, 2015

A. Labbi and A. Mokhnache

formula on the one hand, and on the other hand is to test and validate TAWV retrieval algorithm for the usage in the MSG1-SEVIRI data. The main advantages of our method for remote sensing of the total atmospheric water vapor content from MSG1-SEVIRI observations are the following: it is a physics-based algorithm, it is obtained from the radiance transfer equation, it takes into account only observations in the split-window over varying surface temperatures and it is totally operational.

To estimate and validate TAWV, we have first used the "Roberts" approach to create a relationship between $(\tau_{12}/\tau_{10.8})$ and TAWV. Then, we used the radiance transfer equation to extract the TAWV as a function of $(\tau_{12}/\tau_{10.8})$. Next, a comparison with the TAWV measured by both radiosoundings and aerosol robotic network (AERONET) was made to validate our proposed algorithm. Finally, we gave an example of mapping the TAWV by using only MSG1-SEVIRI data.

2 Data and study area

2.1 TIGR dataset

To simulate the atmospheric transmittance between the surface and the sensor representing a worldwide set of atmospheric situations, the Thermodynamic Initial Guess Retrieval (TIGR) dataset and the Spinning Enhanced Visible and Infrared Imager (SEVIRI) spectral library were used. The TIGR dataset (in version TIGR2000_v1.1) is used in this work. The TIGR dataset was developed at the Laboratoire de Meteorologie Dynamique (LMD, Paris) especially for the development of retrieval methods. TIGR is a climatological library of 2311 representative atmospheric situations. Each situation is described, from the surface to the top of the atmosphere, by the values of the temperature, water vapor and ozone concentrations on a given pressure grid. These atmospheric situations are stratified by a hierarchical ascending classification into five air-mass types: (1) tropical (1–872), (2) mid-latitude summer (873–1260), (3) mid-latitude winter (1261–1614), (4) polar summer (1615–1718) and (5) polar winter (1719–2311).

2.2 Radiosonde and AERONET data

The department of atmospheric sciences of University of Wyoming has a radiosonde database for the whole world. It includes radiosonde observations in 2006 of 10 selected sites (Table 1 and Fig. 1) which were used in this work to compute TAWV and to validate our results. These radiosonde data launched at meteorological stations of the selected sites, provided by the University of Wyoming College of Engineering Department of Atmospheric Science, are available to public users and are available on-line at (http://weather.uwyo.edu/upperair/sou-nding.html). Also, the TAWV measured in 2006 from 4 selected sites (Table 1 and Fig. 1) by the AERONET is used in this work to validate our results. The AERONET is a network of ground-based sun photometers which measure atmospheric aerosol properties and also the TAWV, this project is started by NASA Earth Observing System and expanded by federation with many non-NASA institutions.

2.3 Satellite data and Study area

The thermal infrared data used in this study for estimating TAWV have been acquired by SEVIRI on board MSG1. MSG1 is a geostationary meteorological satellite developed by the European Space Agency (ESA) and the European Organization for the Exploitation of Meteorological Satellites (EUMETSAT) which was successfully put into orbit on 2002 (Jiang, 2007; Julien, 2008). The MSG1 satellite is greatly improved compared to the first generation Meteosat. Those improvements include better spatial and temporal resolution for thermal infrared channels which are 3 km and 15 min respectively. MSG1-SEVIRI provides images with twelve channels, eight of the channels are in the thermal infrared, three in the visible and one of the channels is called the High Resolution Visible (HRV) channel (Julien, 2008). In this work, TAWV was retrieved from clear sky images in the two thermal infrared channels IR10.8 and IR12. The images were acquired at approximately 09:00 and 12:00 UTC in 2006. The study area covers

North Africa, the Mediterranean basin and Southern Europe (see Fig. 1). It contains different types of surface: sea surface, soil surface and vegetation surface.

3 Methodology

3.1 Split-window technique

The split-window technique was originally derived to estimate land surface temperature, specifically sea surface temperature. However, this technique can be extended to the retrieval of the total atmospheric water vapor content (Schroedter-Homscheidt et al., 2008; Kleespies and McMillin, 1990). The split-window technique exploits the difference in water vapor absorption between the 10.8 and the 12 µm channels. In this paper we present a modified split-window algorithm can be used to estimate TAWV with a minimum of a priori information. If we consider the case of a cloudless region where the atmosphere is homogeneous, when the radiative transfer equation is written for two observing conditions under which the surface temperature changes measurably, Kleespies and McMillian (1990), have shown that the ratio of the brightness temperature difference at the two wavelengths (IR10.8 and IR12) is equal to the ratio of the transmittances, that is:

$$\frac{\tau_{12}}{\tau_{10.8}} = \frac{T_{12}^{a} - T_{12}^{b}}{T_{10.8}^{a} - T_{10.8}^{b}}, \tag{1}$$

where τ is the total atmospheric transmittance, T is the brightness temperature, the subscripts refer to the nominal 10.8 and 12 µm channels of the split-window, and the superscripts a and b refer to two observing conditions under which the surface temperature changes measurably, MSG can provide these two observing conditions with varying surface temperatures but a constant viewing geometry during the daily temperature cycle over land.

AMTD
8, 8903–8923, 2015

Then, the relationship between transmittance ratio and TAWV can be determined by synthetic regression and can be written as follows (Schroedter-Homscheidt et al., 2008):

$$W = fct\left(\frac{T_{12}^{a} - T_{12}^{b}}{T_{10.8}^{a} - T_{10.8}^{b}}\right), \tag{2}$$

where W is the TAWV ($\mathrm{g\,cm^{-2}}$).

3.2 Atmospheric transmittance calculation

In this work, we have used a simple technique for atmospheric transmittance calculation in thermal infrared region between 8 and 13 µm, which is based upon a temperature-compensated water vapor continuum function described by Roberts et al. (1976). The monochromatic transmittance for an atmospheric layer was calculated by the formula:

$$\tau_{\lambda} = \exp\left(-\frac{\sigma_{\lambda} z}{\cos\theta}\right), \tag{3}$$

where θ is the satellite sensor zenith angle, z is nadir view path length and σ_{λ} is the water vapor absorption coefficient given by Roberts et al. (1976), and has been rewritten here in terms of wavelength and SI units as follows:

$$\sigma_{\lambda} = \rho[e + 0.002(P - e)]\left[0.004124 + 5.509\exp\left(\frac{-78.7}{\lambda}\right)\right]\exp\left[1800\left(\frac{1}{T} - \frac{1}{296}\right)\right], \tag{4}$$

where ρ is water vapor density ($\mathrm{kg\,m^{-3}}$), e is the water vapor pressure component (kPa), P is the atmospheric pressure (kPa), λ is the wavelength (µm) and T is the atmospheric temperature (K).

AMTD
8, 8903–8923, 2015

A. Labbi and A. Mokhnache

On the one hand, the total monochromatic transmittance of the atmosphere has been calculated by multiplying the transmittances of the different layers of the atmosphere between themselves. On the other hand, the total atmospheric transmittance for the SEVIRI channels has been calculated using the following formula:

$$\tau_i = \frac{\int_{\lambda_1}^{\lambda_2} f_i(\lambda)\tau_\lambda \mathrm{d}\lambda}{\int_{\lambda_1}^{\lambda_2} f_i(\lambda)\mathrm{d}\lambda}, \tag{5}$$

where $f_i(\lambda)$ is the spectral response function of channel i.

In all the following, "Roberts" approach will refer to the calculations of the atmospheric transmittance using the water vapor absorption coefficient given by Roberts et al. (1976).

4 Results and validation

4.1 Relationship between transmittance ratio and total atmospheric water vapor content

To find the relationship between transmittance ratio and total atmospheric water vapor content, the following steps were performed:

Firstly, all TIGR humidity profiles were integrated vertically to calculate the true values of TAWV. Figure 2 displays the distribution of these values for 2311 selected atmospheres. These atmospheric profiles represent a world-wide set of atmospheric situations and are obviously credible to derive the relationship between TAWV and $\tau_{12}/\tau_{10.8}$ (subscripts 10.8, 12 denote channel IR10.8 and IR12, respectively).

Secondly, the "Roberts" approach were performed with all TIGR temperature and humidity profiles to simulate the atmospheric transmittance in channels IR10.8 and IR12. The transmittance ratio ($\tau_{12}/\tau_{10.8}$) is then regressed against the TAWV in the atmosphere computed from the 2311 atmospheric profiles. Scatter diagram between

AMTD
8, 8903–8923, 2015

$\tau_{12}/\tau_{10.8}$ and TAWV is shown in Fig. 3 for different viewing angles ($\theta = 0$, 10, 20, 30, 40 and 50°), we found a quadratic formula between them and can be written as follows:

$$W = -12.3514\,r^2 + 6.71773r + 5.76941, \tag{6}$$

where r is the transmittance ratio, it can be calculated as follow:

$$r = \frac{T_{12}^a - T_{12}^b}{T_{10.8}^a - T_{10.8}^b}. \tag{7}$$

4.2 Validation and application

The best way to validate the retrieved atmospheric water vapor content from the MSG1-SEVIRI data of a specific region is to compare with the in situ ground truth measurements. The radiosonde observations from 10 selected sites (described in the data part) are used to compute TAWV and to validate our results in this work. Also, the TAWV measured from 4 selected sites (see the data part) by the AERONET is used to validate the results. In the two previous cases, the validation of TAWV was made using the data from five selected days (15 January, 15 February, 15 March, 15 July and 15 August) in 2006 at 12:00 UTC. For the practical application of the proposed method we used the following assumptions: (1) cloud-free measurement available for a pixel, (2) the input brightness temperatures with a variation larger than approximately 5 K during the daily cycle, we used this assumption because the simulations taking the specified SEVIRI radiometric noise into account showed that a value larger than approximately 5 K is required as minimum brightness temperature difference (Schroedter-Homscheidt et al., 2008), and (3) the transmission ratio is between 0 and 1.

Figure 4 shows the comparison between the TAWV derived from MSG1-SEVIRI data and that measured by the radiosonde. We found acceptable results: the root mean square error (RMSE) equals 0.66 g cm^{-2}, the standard deviation (SD) equals 0.59 g cm^{-2} and the correlation coefficient (R) equals 0.79. Figure 5 shows the comparison between the TAWV derived from MSG1-SEVIRI data and that measured by

AMTD
8, 8903–8923, 2015

Estimating of total atmospheric water vapor content

A. Labbi and A. Mokhnache

the ARONET. We found good results: the RMSE equals 0.42 g cm^{-2}, the SD equals 0.29 g cm^{-2} and the R equals 0.82. We can conclude that the TAWV can be estimated using the MSG1-SEVIRI observations with accuracy acceptable.

The knowledge of TAWV for large areas is strongly required in several applications, for instance in agrometeorology, climatology and environmental studies. The methodology explained in the paper can be applied to the MSG1-SEVIRI images to obtain maps of TAWV. Figures 6 and 7 show the histogram of the TAWV and the map of the TAWV using the method proposed in this work respectively, this for all available pixels in the study area. The data described in these figures were obtained from MSG1-SEVIRI observations on 15 March 2006 at 12:00 UTC, the cloud was set to be white in the map. To demonstrate that the spatial variation of TAWV here is reasonable, we have shown in Fig. 8 the map of the TAWV retrieval using the method proposed by Schroedter-Homscheidt et al. (2008) for all available pixels in the study area, the map was obtained from MSG1-SEVIRI data on 15 March 2006 at 12:00 UTC. These figures show that the TAWV for most pixels in the study area is less than 3 g cm^{-2}.

5 Conclusion

In this paper, we have presented an operational algorithm for evaluating total atmospheric water vapor content from only the MSG1-SEVIRI data over land surfaces. This algorithm is based on a quadratic formula relationship between TAWV and the ratio of the two split-window channel transmittances, ($\tau_{12}/\tau_{10.8}$), this assumption is based on the "Roberts" approach simulations using MSG1-SEVIRI filter response functions for a 2311 atmospheric situations from the TIGR dataset. The TAWV values derived from MSG1-SEVIRI are then compared with both radiosonde and AERONET data (this for different selected sites in the year 2006). The results indicate that the algorithm proposed is capable of estimating W from MSG1-SEVIRI with accuracy acceptable: the comparison with the radiosonde data show that the RMSE equals 0.66 g cm^{-2}, the SD equals 0.59 g cm^{-2} and the R equals 0.79. Also, the comparison with the radiosonde data show that the RMSE equals 0.42 $g\,cm^{-2}$, the SD equals 0.29 $g\,cm^{-2}$ and the R equals 0.82. The comparison with the method proposed by Schroedter-Homscheidt et al. (2008) demonstrates that the spatial variation of TAWV here is reasonable. We can conclude from this study that the TAWV estimated using the MSG1-SEVIRI observations can be used for weather prediction and climate change research.

Acknowledgements. The authors would like to thank the Department of Atmospheric Sciences of the University of Wyoming for the sounding data were obtained from http://weather.uwyo.edu/upperair/sounding.html. We also wish to thank the PI investigators and their staff for establishing and maintaining the sites used in this investigation.

References

Anding, D. and Kauth, R.: Estimation of Sea Surface Temperature from Space, Remote Sens. Environ., 1, 217–220, 1970.

Czajkowski, K. P., Goward, S. N., Shirey, D. and Walz, A.: Thermal remote sensing of near-surface water vapor, Remote Sens. Environ., 79, 253–263, 2002.

Dalu, G.: Satellite remote sensing of atmospheric water vapour, Int. J. Remote Sens., 7, 1089–1097, 1986.

Goward, S. N., Waring, R. H., Dye, D. G. and Yang, J.: Ecological remote sensing at OTTER: macroscale satellite observations, Ecol. Appl., 4, 322–343, 1994.

Jedlovec, G. J.: Precipitable water estimation from high-resolution split window radiance measurement, J. Appl. Meteorol., 29, 863–877, 1990.

Jiang, G. M.: Retrievals of land surface emissivity and land surface temperature from MSG1-SEVIRI data, Doctoral thesis, Louis Pasteur University, Strasbourg, France, order no.: 5486, 2007.

Julien, Y.: Vegetation monitoring through retrieval of NDVI and LST time series from historical databases, PhD dissertation, Facultat de Física, universitat de València, Spain, 2008.

Kleespies, T. J. and McMillin, L. M.: Retrieval of precipitable water from observations in the split-window over varying surface temperatures, J. Appl. Meteorol., 29, 851–862, 1990.

Morales-Salinas, L., Parra-Aravena, J. C., Lang-Tasso, F., Abarca-Del Río, R., and Jorquera-Fontena, E.: Simple linear algorithm to estimate the space-time variability of precipitable water in the Araucanía Region, Chile, J. Soil Sci. Plant Nutrition, 12, 295–302, 2012.

Price, J. C.: Estimating Surface Temperatures from Satellite Thermal Infrared Data–A Simple Formulation for the Atmospheric Effect, Remote Sens. Environ., 13, 353–361, 1983.

Roberts, R. E., Selby, J. E., and Biberman, L. M.: Infrared continuum absorption by atmospheric water vapor in the 8–12 µm window, Appl. Opt., 15, 2085–2090, 1976.

Schroedter-Homscheidt, M., Drews, A., and Heise S.: Total water vapor column retrieval from MSG-SEVIRI split-window measurements exploiting the daily cycle of land surface temperatures, Remote Sens. Environ., 112, 249–258, 2008.

Sobrino, J. A., Jimenez, J. C., Raissouni, N., and Soria, G.: A Simplified Method for Estimating the Total Water Vapor Content Over Sea Surfaces Using NOAA-AVHRR Channels 4 and 5, IEEE Yrans. Geosci. Remote Sens., 40, 357–361, 2002.

Zhang, T., Wen, J., Velde, R., Meng, X., Li, Z., Liu, Y., and Liu, R.: Estimation of the total atmospheric water vapor content and land surface temperature based on AATSR thermal data, SENSORS, 8, 1832–1845, 2008.

AMTD

8, 8903–8923, 2015

Estimating of total atmospheric water vapor content

A. Labbi and A. Mokhnache

Table 1. Geographic information of the selected sample sites.

Site No.	Name	Latitude	Longitude	Elevation (m)
		Radiosonde sites		
1	Madrid	40.50° N	03.58° W	633
2	Nimes Courbessac	43.86° N	04.40° E	62
3	Milano	45.43° N	09.28° E	103
4	Dar El Beida	36.68° N	03.21° E	29
5	Bechar	31.50° N	02.25° W	816
6	Tindouf	27.70° N	08.16° W	439
7	In Salah	27.23° N	02.50° E	269
8	Tamanrasset	22.78° N	05.51° E	1378
9	Dakar	14.73° N	17.50° W	24
10	Niamey	13.48° N	02.16° E	227
		AERONET sites		
11	Blida	36.51° N	02.88° E	230
12	Ras El Ain	31.67° N	07.60° W	570
13	Agoufou	15.35° N	01.48° W	305
14	IER Cinzana	13.28° N	05.93° W	285

Discussion Paper | Discussion Paper | Discussion Paper | Discussion Paper |

AMTD

8, 8903–8923, 2015

Estimating of total atmospheric water vapor content

A. Labbi and A. Mokhnache

Title Page

Abstract Introduction

Conclusions References

Tables Figures

Back Close

Full Screen / Esc

Printer-friendly Version

Interactive Discussion

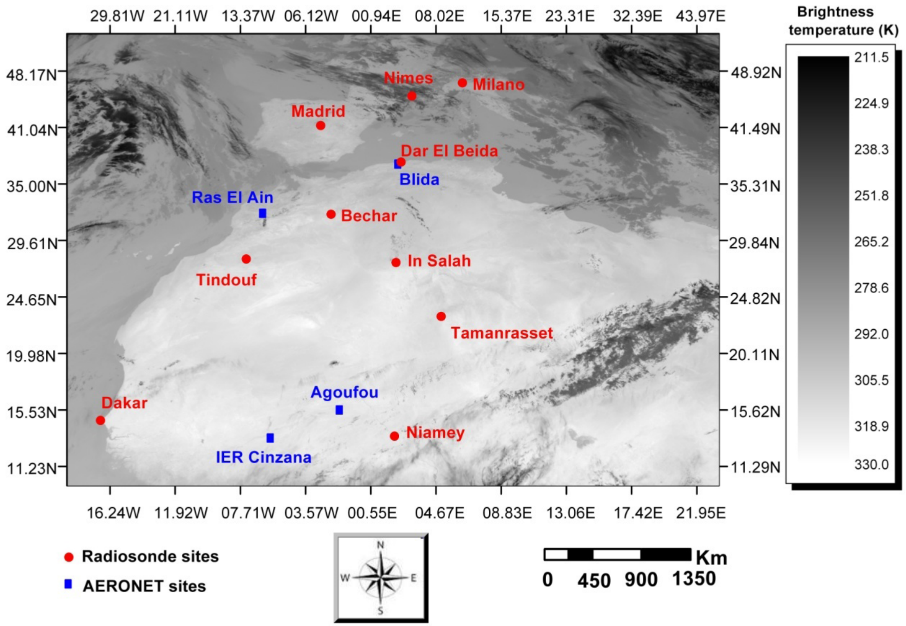

Figure 1. Study area map and the selected sample sites from MSG1-SEVIRI image in IR12 channel, 15 March 2006 at 12:00 UTC.

AMTD
8, 8903–8923, 2015

Title Page
Abstract | Introduction
Conclusions | References
Tables | Figures
◂ | ▸
Back | Close
Full Screen / Esc
Printer-friendly Version
Interactive Discussion

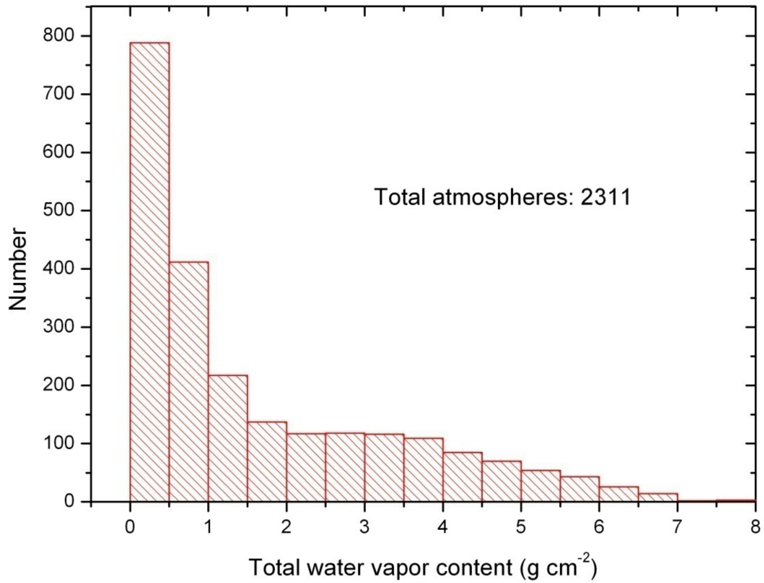

Figure 2. Histogram of the total atmospheric water vapor content in the 2311 atmospheric profiles of the TIGR database.

AMTD
8, 8903–8923, 2015

Estimating of total atmospheric water vapor content

A. Labbi and
A. Mokhnache

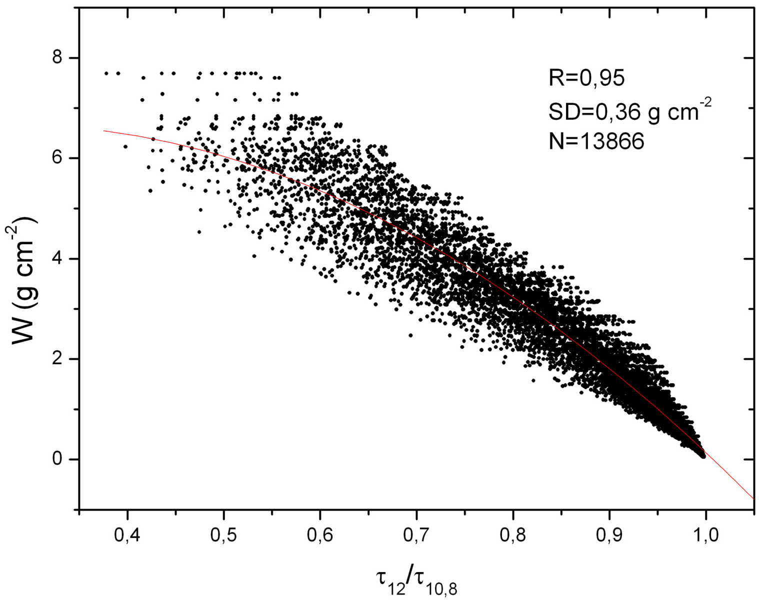

Figure 3. Total atmospheric water vapor content plotted as a function of the transmittance ratio, $\tau_{12}/\tau_{10.8}$, for MSG1-SEVIRI at different viewing angles (θ = 0, 10, 20, 30, 40 and 50°).

AMTD
8, 8903–8923, 2015

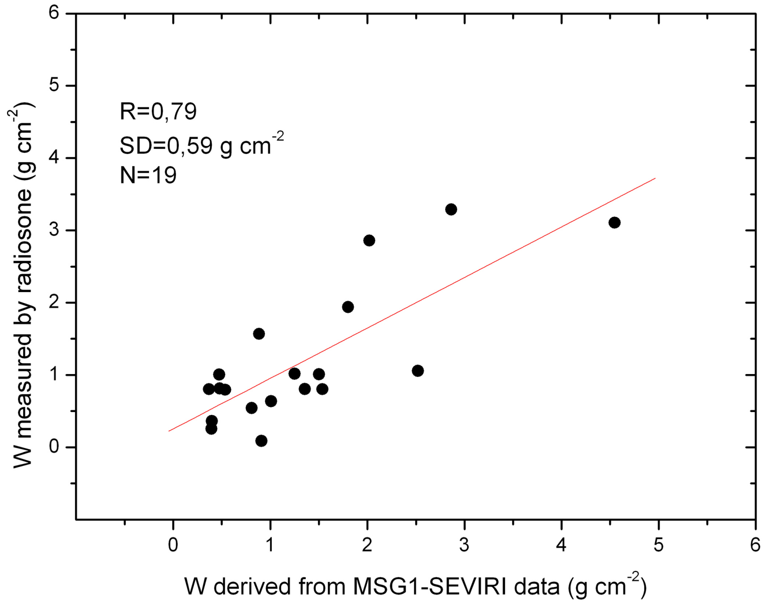

Figure 4. Comparison between the total atmospheric water vapor contents derived from MSG1-SEVIRI data and that measured by the radiosonde.

AMTD
8, 8903–8923, 2015

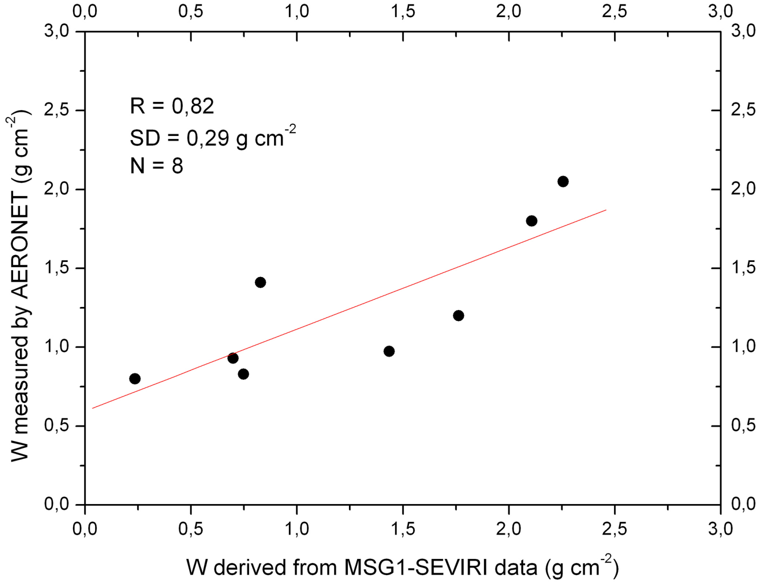

Figure 5. Comparison between the total atmospheric water vapor contents derived from MSG1-SEVIRI data and that measured by AERONET.

AMTD

8, 8903–8923, 2015

A. Labbi and A. Mokhnache

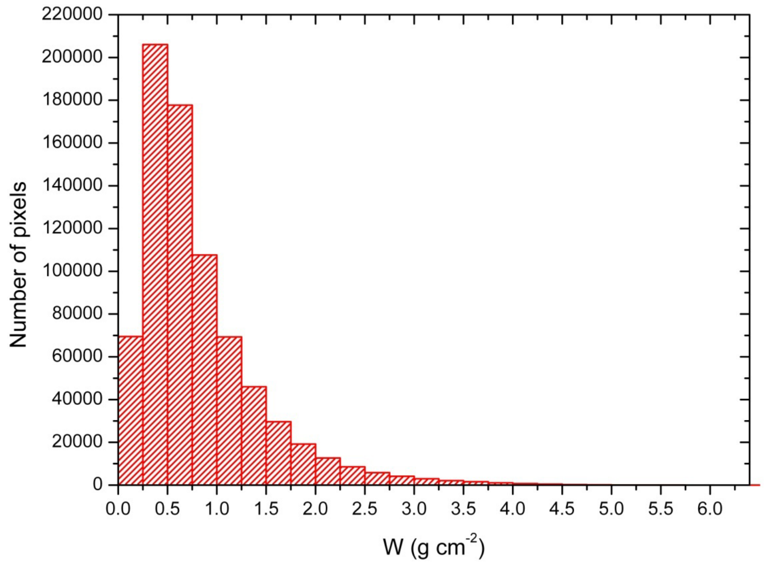

Figure 6. Histogram of the total atmospheric water vapor content using the method proposed in this work for all available pixels in the study area, the histogram was obtained from MSG1-SEVIRI data on 15 March 2006 at 12:00 UTC.

AMTD

8, 8903–8923, 2015

Estimating of total atmospheric water vapor content

A. Labbi and A. Mokhnache

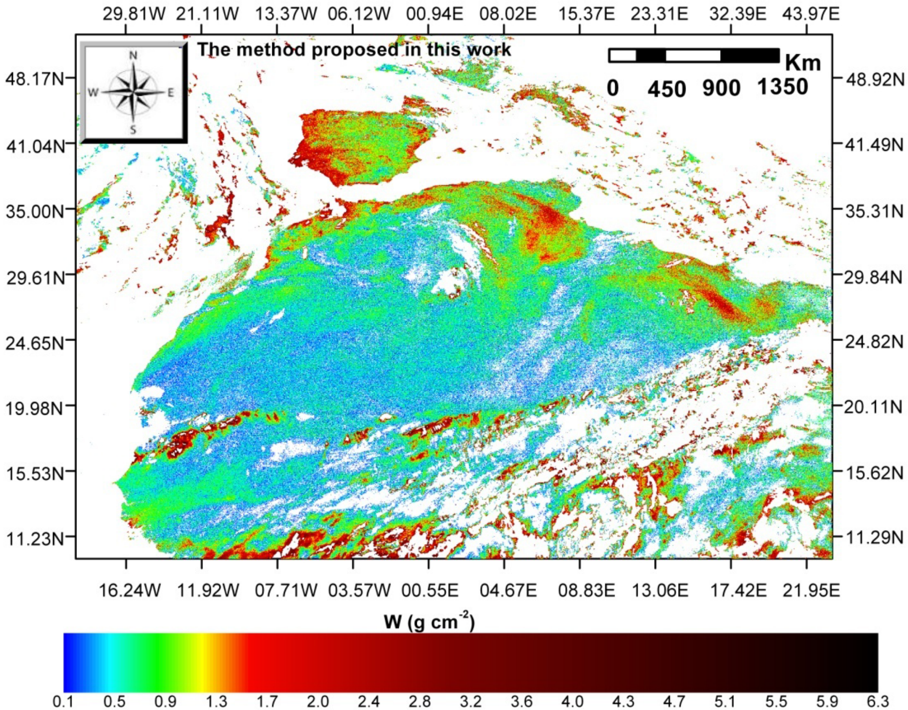

Figure 7. Map of the total atmospheric water vapor content using the method proposed in this work for all available pixels in the study area, the map was obtained from MSG1-SEVIRI data on 15 March 2006 at 12:00 UTC. Cloud was set to be white in the map.

AMTD
8, 8903–8923, 2015

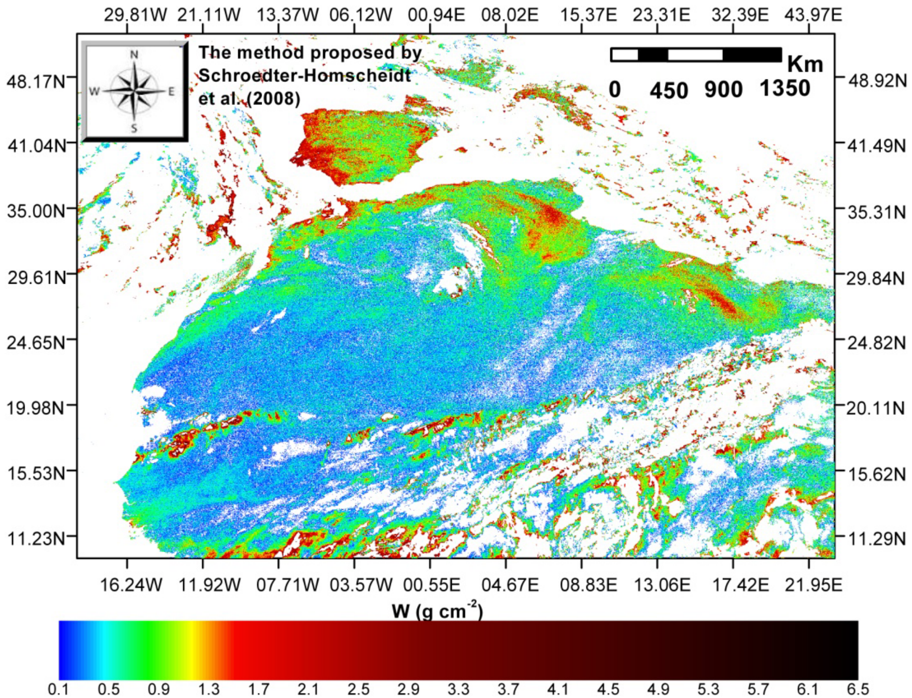

Figure 8. Map of the total atmospheric water vapor content retrieval using the method proposed by Schroedter-Homscheidt et al. (2008) for all available pixels in the study area, the map was obtained from MSG1-SEVIRI data on 15 March 2006 at 12:00 UTC. Cloud was set to be white in the map.

AMTD
8, 8903–8923, 2015

Estimating of total atmospheric water vapor content

A. Labbi and A. Mokhnache